ELSEVIER

Determination of polydimethylsiloxane–seawater distribution coefficients for polychlorinated biphenyls and chlorinated pesticides by solid-phase microextraction and gas chromatography–mass spectrometry

Eddy Y. Zeng[a],*, David Tsukada[b], James A. Noblet[c], Jian Peng[b]

[a] State Key Laboratory of Organic Geochemistry, Guangzhou Institute of Geochemistry, Chinese Academy of Sciences,
P.O. Box 1131, Guangzhou 510640, China
[b] Southern California Coastal Water Research Project, 7171 Fenwick Lane, Westminster, CA 92683, USA
[c] Department of Chemistry, California State University, San Bernardino, CA 92407, USA

Abstract

Applications of solid-phase microextraction (SPME) in the measurement of very hydrophobic organic compounds (VHOCs) are limited, partly due to the difficulty of calibrating SPME fibers for VHOCs. This study used a static SPME strategy with a large sample volume (1.6 L) and a five-point calibration procedure to determine the distribution coefficients for a large suite of polychlorinated biphenyls (PCBs) and chlorinated pesticides between a polydimethylsiloxane (PDMS) phase (100 μm thickness) coated on a glass fiber and seawater. An extraction time of 12 days was deemed adequate for equilibrium calibration from kinetic experiments. Two groups of randomly selected fibers divided into three batches (up to nine fibers in each batch) were processed separately with two gas chromatography–mass spectrometry (GC–MS) systems. Matrix effects arising from losses of the analytes to glass container walls and stirring bars were corrected. Relative standard deviations within the same batch were generally smaller than those for the entire group. Furthermore, $K_f V_f$ (K_f and V_f are the distribution coefficient of an analyte between the polymer-coated fiber and aqueous phase and the fiber volume, respectively) values determined with two GC–MS systems were statistically different. These results indicate the calibrated $K_f V_f$ values were less affected by the random selection of SPME fibers than by other experimental conditions, and therefore average $K_f V_f$ values may be used for the same type of commercially available SPME fibers. The relative accuracy of our calibration method was similar to that of a previous study [P. Mayer, W.H.J. Vaes, J.L.M. Hermens, Anal. Chem. 72 (2000) 459] employing different coating thickness and calibration procedure. The present study also obtained a bell-shaped relationship between log K_f and log K_{ow} (octanol–water partition coefficient) for PCB congeners with the maximum log K_f corresponding to log $K_{ow} \sim 6.5$. This bell-shaped relationship was attributed mainly to steric effects arising from the interplay between the PDMS thickness and molecular sizes of the target analytes.
© 2005 Elsevier B.V. All rights reserved.

Keywords: Solid-phase microextraction; Partition coefficient; Hydrophobic organic compound; Calibration

1. Introduction

Since the introduction of solid-phase microextraction (SPME) as a quantitative analytical technique by Arthur and Pawliszyn [2] more than a decade ago, a large amount of data

has been accumulated concerning the fundamental mechanisms governing the SPME processes and potential applications of SPME in a variety of research areas [3–6]. Successful implementation of a feasible SPME-based method is strongly dependent upon an accurate determination of K_f values between the SPME sorbent phase and sample matrix. While K_f values for volatile organic compounds are relatively easy to determine with precision, quantifying K_f values for very

hydrophobic organic compounds (VHOCs) has remained a difficult task.

Two general calibration methods have been employed to determine K_f values for VHOCs. The first one is a static SPME procedure within a closed system where single- and multi-point calibration strategies have been attempted. For single-point calibration, the following equation or equivalent has been derived to calculate K_f [7,8]:

$$K_f = \frac{N_f V_w}{V_f (C_w^0 V_w - N_f)} \quad (1)$$

where K_f and V_f are defined in the abstract, N_f is the analyte amount in the polymer phase coated on a SPME fiber, V_w is the water volume, and C_w^0 is the initial analyte concentration in water. One apparent drawback with this method is the possible occurrence of large measurement errors if the analyte amount (N_f) in the sorbent phase is approaching the initial analyte amount ($C_w^0 V_w$). Mayer et al. [1] proposed a multi-point calibration strategy, in which a series of samples with the same analyte concentration were prepared with different amounts of polydimethylsiloxane (PDMS)-coated fibers to obtain varying PDMS to water volume ratios (V_f/V_w). A reference sample without addition of PDMS-coated fibers was also processed. The ratio ($C_{relative}$) of the analyte concentrations in the treated and reference samples was related to V_f/V_w via the following equation [1]:

$$C_{relative} = \frac{1}{1 + 10^{\log K_f} (V_f / V_w)} \quad (2)$$

A nonlinear regression between $C_{relative}$ and V_f/V_w yields the distribution coefficient K_f. In this approach, the analyte concentrations in the treated samples were not measured in situ; instead, subsamples were collected into 12-mL vials and extracted with conventional SPME.

The second calibration method is dynamic SPME in which a constant analyte concentration is maintained by an external source so that losses of analytes to non-SPME sorbent phases can be disregarded [7,9]. In this approach, K_f is calculated directly from $K_f = C_f/C_w$. However, the analyte concentration, C_w, in the sample needs to be determined by a separate analytical protocol, typically a liquid–liquid extraction method. As a result, the accuracy of the K_f values is also subject to the performance of a non-SPME method.

Our applications of the SPME technology include field sampling of VHOCs in oceanic environments [10], which requires determination of K_f values for a large number of analytes and SPME fibers of maximum capacity (100 μm PDMS-coated fibers in this study). So far, K_f values have been determined for only a small number of polychlorinated biphenyl (PCB) and DDT compounds with PDMS-coated fibers [1,7,8,11–13]. In addition, the two calibration methods described above become impractical when a large number of SPME fibers are calibrated. In view of these issues, a new analytical protocol was used in this study to calibrate a large set of PDMS-coated fibers for selected PCB congeners and chlorinated pesticides that are normally measured in southern

California ocean monitoring programs, such as a recent regional survey [14]. The protocol involves a five-point (including the origin) calibration approach that is widely employed in other conventional analytical methods, as well as correction for sorption of the analytes to the two major non-SPME sorbent phases in the experimental set-up; the glass container walls and stirring bar surfaces. One objective of the present study was to determine the intra- and inter-batch variability of K_f values and assess whether an average K_f value from a large pool of SPME fibers could be used in quantitation of a specific analyte. Another objective was to examine the variability of K_f values obtained from two analytical instruments. This is important, as multiple analytical instruments are often needed for sample analysis with large-scale sampling programs. Finally, the results from the present study were compared with those from several previous studies to understand factors affecting the calibration of SPME fibers for VHOCs.

2. Methods

2.1. Theory

In this study, we adopted a static calibration strategy with a large sample volume (1.6 L) and multiple SPME fibers. As required by mass balance, the amounts of an analyte distributed among various phases upon equilibrium SPME are related by:

$$N_0 = N_w + N_a + \sum_{i=1}^{n} N_f(i) + \sum_{i'=1}^{n'} N_{sb}(i') \quad (3)$$

where N_a and $N_f(i)$ are the amounts of the analyte in the air phase (i.e., headspace) and sorbed on the ith SPME fiber, n the total number of SPME fibers, $N_{sb}(i')$ the amount of the analyte sorbed on the i'th non-SPME sorbent phase, and n' is the number of non-SPME sorbent phases. Using the same procedure described previously [15], the amount of the analyte sorbed on the jth SPME fiber is given by:

$$N_f(j) = \frac{K_f V_f}{K_f V_f + V_w + \theta + K_H' V_a} \left(N_0 - \sum_{i \neq j}^{n} N_f(i) \right) \quad (4)$$

where θ, defined as a matrix sorption term [15], accounts for the N_{sb} term in Eq. (3) and will be further discussed below, K_H' is the dimensionless Henry's Law constant ($= K_H/RT$, where K_H is the Henry's Law constant, R is the universal gas constant, and T is the absolute temperature), and V_a is the headspace volume. If S is defined as the slope of the linear regression of $N_f(j)$ versus $(N_0 - \sum_{i \neq j}^{n} N_f(i))$, the following equation can be derived:

$$K_f V_f = \frac{S(V_w + \theta + K_H' V_a)}{1 - S} \quad (5)$$

Apparently, the present analytical method was developed directly from the linearity between the analyte amount retained by an SPME fiber and the initial analyte amount minus the analyte amounts retained by all other SPME fibers. Linear regression over a large concentration range (2–50 ng/L in the present study) ensures the wide-range applicability of the measured K_f values. In addition, the use of multiple SPME fibers in one calibration system allows the calibration data to be analyzed statistically. To estimate the value of θ in a given system, we rewrite θ as [15]:

$$\theta = \sum_{i=1}^{n'} K_{sb}^i m_{sb}^i \qquad (6)$$

where K_{sb}^i is the distribution coefficient of the analyte between the ith non-SPME sorbent phase and the aqueous phase and m_{sb}^i is the apparent mass of the ith non-SPME sorbent phase. By definition, $K_{sb}^i = C_{sb}^i / C_w$, where C_{sb}^i is the concentration of the analyte in the ith non-SPME sorbent phase. By substituting this relationship into Eq. (6) and noting $N_{sb}(i) = C_{sb}^i m_{sb}^i$, we may obtain $\sum_{i=1}^{n'} N_{sb}(i) = \theta C_w$ or more conveniently,

$$\sum_{i=1}^{n'} N_{sb}(i) = \left(\frac{\theta}{V_w} \right) N_w \qquad (7)$$

Therefore, θ can be estimated from the linear regression of $\sum_{i=1}^{n'} N_{sb}(i)$ versus N_w and V_w. It is worthwhile to note that because θ is a constant for a given analyte in a specific experiment system $\sum_{i=1}^{n'} N_{sb}(i)$ can be determined under non-SPME conditions. In the present study, the glassware wall and stirring bar surface were the two non-SPME sorbent phases under consideration. Headspace was deemed insignificant compared to other non-SPME sorbent phases under the present experimental conditions, i.e., $K_H' V_a$ was set to zero (more discussion on this issue is given later).

2.2. SPME procedures

The 100 μm PDMS-coated fibers with a coating volume (V_f) of 0.612 μL (Supelco, Bellefonte, PA, USA) were washed with hexane (nanograde; Mallinckrodt Baker, Phillipsburg, NJ, USA) and conditioned at 280 °C under helium stream (on a GC injection port) for 1 h prior to initial use or after each injection. Glass flasks of ~1.7 L (Corning, Corning, NY, USA) were washed with detergent and tap water, rinsed with deionized water, kilned at 420 °C for at least 4 h. Immediately prior to use, each flask was silanized with a solution of 15% dimethyldichlorosilane in toluene (Aldrich, Milwaukee, WI, USA) for ~1 min, rinsed twice with toluene and three times with methanol, dried at 100 °C, and rinsed with deionized water. PTFE-coated stirring bars

(Corning) were rinsed with deionized water, sonicated in methylene chloride (HPLC–GC–MS grade; Fisher Scientific, Pittsburgh, PA, USA) for 20 min, and dried at 100 °C.

Custom-made mixtures of PCB congeners (20 μg/mL each in hexane–isooctane (98:2)) and chlorinated pesticides (100 μg/mL each in acetone) (AccuStandards, New Haven, CT, USA) were diluted with acetone (OPTIMA grade; Fisher Scientific) to make up spiking solutions (in 0.5 mL acetone) with various analyte concentrations. Each Erlenmeyer flask was filled with 1.6 L of sand-filtered seawater (with dissolved organic carbon less than 1 mg/L, salt content of 33.1%, conductivity of 50.0 μS and pH 8.1) and spiked with a spiking solution. One stirring bar was placed in the flask. An antibiotic agent, sodium azide (Mallinckrodt Baker), was added to the flask if the experiment was to be conducted for 4 days or longer. A solvent-washed PTFE sheet was bound to the opening of the flask with rubber bands to make the system airtight. Upon rinse with hexane, multiple SPME fibers were pierced through the PTFE sheet and into the spiked seawater. The PDMS-coated fibers were protracted and exposed to the spiked seawater. The flask was placed on a Corning stirrer. To minimize heat transfer from the stirrer motor to the flask, a 150 mm × 15 mm polystyrene Petri dish with lid was placed between the stirrer and the flask (Fig. 1). All experiments were conducted at ambient temperature 22 ± 2 °C. At the end of the extraction, the PDMS-coated fibers were removed with care from the flask (PTFE sheet around each SPME fiber was cut open to allow the fiber to slide out) and dipped briefly into deionized water to remove residual salt from the seawater. The fibers were then shaken vigorously to remove any water residues before being retracted into the
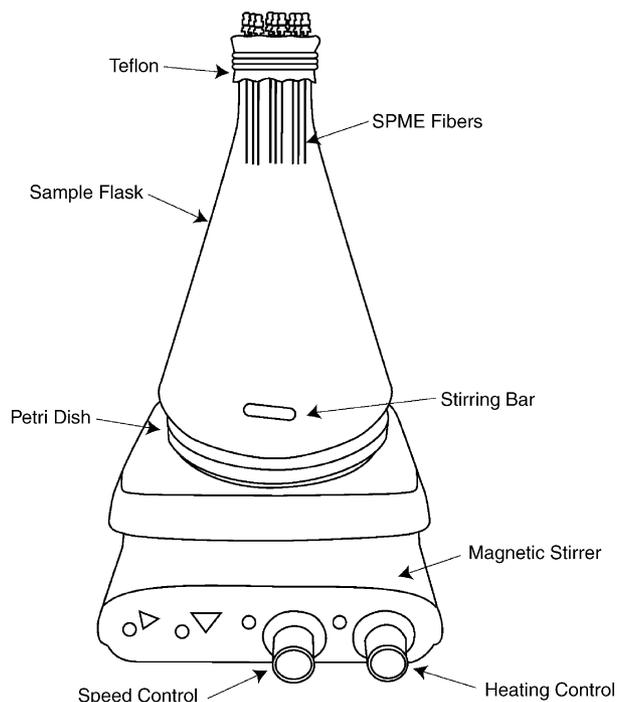

Fig. 1. Schematic of the SPME experimental set-up.

needle sleeves. Analytes sorbed on SPME devices were thermally desorbed into a programmed injector on a specified gas chromatography–mass spectrometry (GC–MS) instrument. SPME fibers were generally processed on the same day when extraction was complete (all within 48 h). SPME fibers not analyzed immediately were stored at $-20\,^{\circ}$C.

For uptake kinetics experiments, three SPME fibers were used simultaneously in one flask with a spiking concentration of 50 ng/L for all analytes. SPME extraction times were 1, 2, 4, 8, and 16 h and 1, 2, 4, 6, 8, 12, 16, and 24 days. Two agitation speeds, 380 and 870 rpm, were tested. For equilibrium calibration experiments, an extraction time of 12 days and an agitation speed of 870 rpm were chosen, based on the results of the kinetics experiments, to determine K_f values. Nine SPME devices were placed in one flask (as one batch), and a total of six batches of fibers were processed. The calibration concentrations were 2, 5, 20, and 50 ng/L for all target analytes.

2.3. Non-SPME procedures

To determine the θ values, four seawater samples (1.6 L) containing the target analytes at 100, 250, 500, and 1000 ng/L, respectively, were prepared in three Erlenmeyer flasks. One stirring bar was placed in each flask and the samples were treated as those with the SPME procedures, except that no SPME fibers were added. At the end of the 12-day extraction, seawater was processed with a solid-phase extraction method [16], stirring bars were extracted with a roller table method [17], and the glassware walls were rinsed with methylene chloride and the rinsates were collected. All fractions were concentrated to 1 mL using a Zymark TurboVap 500 (Zymark Corporation, Hopkinton, MA). Internal standards, PCB 30 and PCB 205, were added to all extracts prior to instrumental analysis.

2.4. GC–MS analysis

Two Varian Saturn 2000 GC/ion trap-MS systems (Walnut Creek, CA, USA) were used for sample analysis, labeled as GC–MS-1 and GC–MS-2. To maintain consistency, all SPME fibers used in the kinetics experiments were analyzed using GC–MS-1. SPME fibers from the equilibrium experiments were categorized into analytical batches 1–6. Fibers in batches 1–3 were analyzed with GC–MS-1, and those in batches 4–6 were analyzed with GC–MS-2. The chromatographic conditions used for these two instruments were identical except for the carrier gas flow rates. Chromatographic separation was made with 60 m $\times$ 0.25 mm I.D. (0.25 μm film thickness) DB-5MS columns (J&W Scientific, Folsom, CA, USA). Column temperature was programmed from 80 $^{\circ}$C (hold for 1 min) to 176 $^{\circ}$C at a rate of 8 $^{\circ}$C/min, followed by a ramp to 230 $^{\circ}$C at a rate of 1.5 $^{\circ}$C/min, and finally increased to 290 $^{\circ}$C (5 $^{\circ}$C/min), where it was held for 21 min. Both SPME and direct solvent injections were conducted with a split/splitless mode (split initially, splitless

0.01 min after injection, and split again 2.5 min after injection). The injector temperature was programmed from 100 $^{\circ}$C (held for 0.05 min) to 280 $^{\circ}$C with the maximum ramping rate ($\sim$100 $^{\circ}$C/min) and held for 40 min at 280 $^{\circ}$C. Under these chromatographic conditions, slightly different retention times were obtained on the two instruments for the same target analytes. To reduce the retention time difference, the flow rate was set at 1.0 and 1.3 ml/min for GC–MS-1 and GC–MS-2, respectively. All the extracts obtained from the non-SPME procedures were analyzed with GC–MS-1.

Mass spectra were acquired with the electron ionization mode. Mass spectra were acquired from 100 to 504 m/z with a scan time of 0.7 scans per second and an emission current of 15 μA. Within this range, ion storage level was 79 and ionization time factor was 100%. Ionization time factor was 10% outside this range. Electron multiplier voltage was 1900–2000 eV for GC–MS-1 and 1500–1600 eV for GC–MS-2, because a newer electron multiplier was installed in GC–MS-2. Temperatures of ion trap, manifold, and transfer line were set at 200, 80, and 280 $^{\circ}$C, respectively. To ensure the linearity of the instrument performance, calibration standard solutions containing all the target analytes at 50, 100, 250, 500, 1000, and 2000 ng/mL with internal standards at 500 ng/mL were analyzed frequently throughout the study. Linear calibration curves were always obtained with high confidence ($r^2 > 0.99$) for all target analytes.

2.5. Data analysis

2.5.1. Normalization of MS responses
An external calibration method was used in the present study. Prior to analysis of each batch of up to seven loaded SPME fibers, 1 μL of a standard mixture containing all the target analytes at 2 μg/mL was injected into the GC–MS instrument with an autosampler. The MS responses from the direct injection of the standard solution and desorption of analytes sorbed on SPME fibers were used to calculate either normalized responses for the kinetics study or analyte amounts for the equilibrium experiments.

2.5.2. Kinetic data
A typical SPME process is believed to occur via a first-order diffusion of an analyte across the polymeric coating–water interface. The amount (N_f) of the analyte sorbed in the PDMS phase may be related to extraction time (t) through the following equation [18]:

$$N_f = N_f^{\infty}(1 - e^{-bt}) \tag{8}$$

where N_f^{∞} is the amount of the analyte sorbed on the SPME fiber at equilibrium ($t \rightarrow \infty$), and b is a kinetic constant related to the type of polymeric coating, analyte and sample volume [18]. In the context of sorption and desorption involved in a diffusion process, b can also be regarded as the rate of desorption from the sorbent phase to the aqueous phase. Eq. (8) can be rearranged to estimate the percent of equilibrium

state (defined as P_{ES}) with finite extraction time t:

$$P_{ES} = (1 - e^{-bt}) \times 100\% \qquad (9)$$

Finally, Eq. (5) can be modified by addition of a time factor under nonequilibrium conditions:

$$K_f V_f = \frac{S(V_w + \theta)}{1 - e^{-bt} - S} \qquad (10)$$

3. Results and discussion

3.1. Kinetics of SPME process

The SPME process was simulated reasonably well with a first-order diffusion model depicted by Eq. (8). The correlation coefficients for the model simulation were largely about 0.7 (Table 1), indicating a fair amount of variability in the kinetic experiments. Since different PDMS-coated fibers were used at different time points in the experiments, the variability may partially reflect differences in the sorptive capacity among individual fibers.

The N_f^∞ values increased for congeners with up to five chlorines, and then decreased for PCBs with six chlorines and above. On the other hand, b essentially decreased with increasing congener number. As a result, the percent of equilibrium state (P_{ES}) calculated with Eq. (9) at 12 days generally decreased with increasing congener number (Table 1). However, the P_{ES} values at 12 days were greater than 80% for all analytes but PCB 209. In general, chlorinated pesticides reached higher percent of equilibrium state than PCBs under the experimental conditions. In the equilibrium experiments, an extraction time of 12 days was used. Because of the moderate variability of the data set, there was no need to include the extraction time factor (Eq. (10)) in the determination of $K_f V_f$ values.

As stated previously, one objective of this study was to develop a feasible field sampling method based on the SPME technology. Consequently, the agitation speed was set to simulate the speed of bottom currents in the coastal ocean of southern California. A previous study obtained the near-bottom current speeds at ∼5–6 cm/s around the coastal oceans off southern California [19]. The agitation velocity in water, labeled as $u(r)$, could be estimated with the following equation [3]:

$$u(r) = 0.575\pi N R^2 \frac{1}{r} \quad \text{for} \quad r > 0.74R \qquad (11)$$

where R is the radius of the stir bar, N is the revolutions per second, and r is the distance between the center of the container and the PDMS-coated fiber. The agitation velocity (870 rpm) in our experiments estimated from Eq. (11) was about 4 cm/s. Note that Eq. (11) is applicable to cylindrical containers, whereas the flasks used in our experiments are pear-shaped. As the PDMS-coated fibers were positioned at the smaller end of the flask (Fig. 1), the agitation veloc-

Table 1
Kinetic parameters associated with SPME processes based on Eqs. (8) and (9)[a]

Analyte	r^2	N_f^{∞} [b]	b (h^{-1})	P_{ES} (%)[c]
PCB 18	0.84	146 (6)	0.0273 (0.0046)	100
PCB 28	0.73	195 (14)	0.0177 (0.0050)	99
PCB 37	0.64	213 (18)	0.0195 (0.0063)	100
PCB 44	0.77	366 (32)	0.0096 (0.0026)	94
PCB 49	0.76	360 (33)	0.0090 (0.0026)	93
PCB 52	0.76	352 (31)	0.0096 (0.0027)	94
PCB 65	0.74	332 (31)	0.0097 (0.0030)	94
PCB 66	0.70	351 (36)	0.0098 (0.0032)	94
PCB 70	0.74	377 (38)	0.0091 (0.0026)	93
PCB 74	0.74	335 (32)	0.0091 (0.0027)	93
PCB 77	0.72	348 (34)	0.0103 (0.0030)	95
PCB 81	0.73	363 (35)	0.0099 (0.0033)	94
PCB 87	0.74	429 (49)	0.0068 (0.0023)	86
PCB 99	0.73	372 (45)	0.0066 (0.0023)	85
PCB 101	0.73	420 (50)	0.0066 (0.0024)	85
PCB 105	0.71	383 (44)	0.0074 (0.0026)	88
PCB 110	0.72	432 (50)	0.0071 (0.0025)	87
PCB 114	0.71	344 (40)	0.0073 (0.0027)	88
PCB 118	0.75	346 (40)	0.0068 (0.0022)	86
PCB 119	0.71	373 (47)	0.0068 (0.0025)	86
PCB 123	0.70	338 (42)	0.0069 (0.0025)	86
PCB 126	0.69	366 (44)	0.0086 (0.0029)	92
PCB 128	0.70	277 (38)	0.0064 (0.0024)	84
PCB 138	0.68	283 (39)	0.0063 (0.0025)	84
PCB 149	0.68	312 (45)	0.0063 (0.0025)	84
PCB 151	0.67	338 (55)	0.0065 (0.0024)	85
PCB 153/168	0.62	223 (33)	0.0071 (0.0032)	87
PCB 156	0.73	246 (30)	0.0068 (0.0023)	86
PCB 157	0.77	225 (25)	0.0065 (0.0019)	85
PCB 158	0.60	220 (34)	0.0079 (0.0033)	90
PCB 167	0.75	209 (26)	0.0062 (0.0020)	83
PCB 169	0.76	197 (21)	0.0073 (0.0020)	88
PCB 170	0.69	128 (18)	0.0063 (0.0023)	84
PCB 177	0.64	159 (25)	0.0061 (0.0027)	83
PCB 180	0.72	137 (19)	0.0060 (0.0021)	82
PCB 183	0.65	134 (23)	0.0063 (0.0024)	84
PCB 187	0.66	152 (26)	0.0062 (0.0024)	83
PCB 189	0.73	122 (16)	0.0061 (0.0020)	83
PCB 194	0.72	68 (9)	0.0060 (0.0018)	82
PCB 200	0.66	63 (9)	0.0068 (0.0024)	86
PCB 201	0.68	72 (10)	0.0063 (0.0023)	84
PCB 206	0.80	37 (4)	0.0066 (0.0018)	85
PCB 209	0.64	25 (6)	0.0038 (0.0018)	66
Aldrin	0.72	428 (52)	0.0068 (0.0024)	86
α-Chlordane	0.74	356 (33)	0.0103 (0.0028)	95
γ-Chlordane	0.74	379 (38)	0.0094 (0.0027)	93
Chlordene	0.80	274 (21)	0.0106 (0.0024)	95
Chloropyrifos	0.58	63 (4)	0.1144 (0.0337)	100
Diazinon	0.21	10 (1)	0.3589 (0.1187)	100
Dieldrin	0.77	129 (6)	0.0469 (0.0091)	100
Endrin	0.55	58 (4)	0.0775 (0.0233)	100
cis-Nonachlor	0.72	331 (32)	0.0108 (0.0032)	96
trans-Nonachlor	0.72	438 (51)	0.0081 (0.0026)	90
Oxychlordane	0.75	332 (29)	0.0102 (0.0030)	95
o,p'-DDD	0.76	314 (25)	0.0119 (0.0030)	97
p,p'-DDD	0.76	275 (19)	0.0160 (0.0039)	99
o,p'-DDE	0.67	439 (58)	0.0075 (0.0029)	89
p,p'-DDE	0.69	435 (62)	0.0070 (0.0026)	87
o,p'-DDT	0.65	353 (53)	0.0065 (0.0028)	84
p,p'-DDT	0.68	407 (59)	0.0078 (0.0031)	89

r^2 is the correlation coefficient for the nonlinear regressions.
[a] The numbers in parentheses are standard errors from the regression analysis of the kinetic data.
[b] Mass spectral abundances of sorbed analytes normalized to those from standard solvent injection.
[c] Calculated at the extraction time of 12 days.

ity based on Eq. (11) was likely underestimated. Therefore, the actual agitation velocity is considered slightly greater than 4 cm/s, but still much slower than those normally used by other researchers. One negative consequence of using a slow-stirring procedure with a large sample volume (1.6 L) is the extended experimental time needed to reach equilibrium. This could allow bacteria to grow, which could biodegrade the analytes. We observed that both o,p'- and p,p'-DDT began to suffer losses after more than 4 days of SPME experiments without the antibiotic agent (sodium azide) added. Therefore, it was necessary to add the antibiotic agent to samples subject to SPME of equal to or longer than 4 days.

In several previous studies, the equilibrium time for SPME of PCBs varied from several hours [11,12] to several weeks [1], depending mainly on the effective agitation velocity around the SPME fiber. As indicated by Eq. (11), the agitation velocity is inversely proportional to the distance between the SPME fiber and the center of the container. Hence, the agitation velocity likely decreases with increasing sample size. It is also beneficial to use stirring bars with a large radius if a large sample container is employed.

3.2. Variability of K_fV_f values

Table 2 summarizes the data acquired from the calibration of the 100 μm PDMS-coated fibers. The log K_f values were

calculated from the K_fV_f data and the V_f value of 0.612 μL was provided by Supelco. The five-point calibration (including the origin) procedure employed to obtain K_fV_f using Eq. (4) appeared valid, as evidenced by generally high r^2 values for a total of 60 analytes. The linear regressions performed to estimate θ values for all the analytes using Eq. (7) were also deemed appropriate since the average r^2 value was 0.88 ± 0.14.

An unexpected occurrence is the significant difference between the K_fV_f values obtained with two seemingly identical GC–MS systems, as indicated by p-values from paired t-tests (Table 2). The target analytes that do not have significant different K_fV_f values obtained with GC–MS-1 and GC–MS-2 are PCB 194, PCB 206, PCB 209, endrin, and o,p'-DDT. Except for o,p'-DDT, K_fV_f values for these compounds are all unexpectedly low (Table 2). As the SPME fibers were randomly selected from a large pool purchased on different days, variability in the sorptive capacity of the commercial PDMS-coated fibers was ruled out as the significant source of the difference. The Corning stirrers were maintained at the same operational mode during the entire experimental period and chosen randomly for specific testing batches. Hence, agitation speed was also ruled out as the main reason for the difference. In quantifying the target analytes desorbed from the PDMS-coated fibers, mass spectral abundances (i.e., area counts) from analysis of solvent

Table 2

Equilibrium properties of polychlorinated biphenyls (PCBs) and chlorinated pesticides on 100 μm PDMS-coated fibers[a]

Analyte	r^{2}[b]		θ (L)[c]	K_fV_f ($\times 10^{-4}$ μL)[d]		p[e]
	Group 1	Group 2		Group 1	Group 2	
PCB 18	0.97 (0.03)	0.97 (0.02)	0.12 (0.00)	7.93 (1.15)	5.67 (1.28)	0.000
PCB 28	0.97 (0.03)	0.96 (0.03)	0.36 (0.06)	10.6 (1.7)	8.22 (2.20)	0.000
PCB 37	0.94 (0.03)	0.95 (0.04)	0.54 (0.16)	12.3 (3.1)	8.57 (2.66)	0.000
PCB 44	0.96 (0.03)	0.94 (0.03)	0.46 (0.01)	19.1 (2.6)	12.8 (4.9)	0.000
PCB 49	0.96 (0.03)	0.94 (0.03)	0.55 (0.10)	20.3 (2.9)	13.3 (4.8)	0.000
PCB 52	0.96 (0.03)	0.94 (0.02)	0.45 (0.05)	19.3 (2.9)	12.8 (4.4)	0.000
PCB 65	0.96 (0.03)	0.92 (0.05)	0.48 (0.08)	23.7 (4.0)	14.6 (5.2)	0.000
PCB 66	0.95 (0.05)	0.92 (0.03)	0.96 (0.10)	23.1 (3.5)	17.5 (7.8)	0.002
PCB 70	0.96 (0.04)	0.93 (0.03)	0.85 (0.13)	20.4 (2.8)	15.5 (6.5)	0.001
PCB 74	0.95 (0.06)	0.93 (0.03)	0.96 (0.24)	20.3 (2.8)	15.7 (6.2)	0.001
PCB 77	0.94 (0.05)	0.91 (0.06)	3.65 (0.04)	39.2 (3.8)	32.9 (15.4)	0.048
PCB 81	0.96 (0.04)	0.88 (0.13)	1.24 (0.09)	25.5 (2.9)	16.5 (8.3)	0.000
PCB 87	0.94 (0.05)	0.89 (0.07)	1.57 (0.29)	23.8 (3.3)	17.8 (8.9)	0.002
PCB 99	0.93 (0.06)	0.88 (0.09)	1.89 (0.53)	22.8 (3.2)	17.2 (8.2)	0.002
PCB 101	0.94 (0.05)	0.89 (0.08)	1.67 (0.39)	25.1 (3.8)	18.2 (8.6)	0.001
PCB 105	0.94 (0.04)	0.90 (0.08)	3.63 (0.68)	33.6 (4.9)	21.3 (6.3)	0.000
PCB 110	0.94 (0.05)	0.89 (0.09)	1.52 (0.31)	23.2 (3.2)	16.2 (7.6)	0.000
PCB 114	0.92 (0.07)	0.88 (0.09)	3.62 (0.70)	29.9 (4.2)	20.0 (8.2)	0.000
PCB 118	0.92 (0.07)	0.88 (0.09)	3.63 (0.69)	28.7 (3.4)	19.5 (6.7)	0.000
PCB 119	0.92 (0.07)	0.84 (0.13)	1.95 (0.47)	23.1 (3.4)	17.3 (8.9)	0.004
PCB 123	0.90 (0.10)	0.87 (0.10)	3.77 (0.62)	28.1 (4.3)	21.3 (10.9)	0.005
PCB 126	0.93 (0.04)	0.90 (0.04)	3.96 (0.59)	32.9 (4.7)	27.2 (12.8)	0.040
PCB 128	0.93 (0.06)	0.88 (0.11)	4.50 (0.41)	21.0 (5.2)	11.9 (4.1)	0.000
PCB 138	0.92 (0.06)	0.89 (0.09)	4.42 (0.52)	19.2 (4.1)	14.3 (6.7)	0.003
PCB 149	0.93 (0.05)	0.87 (0.12)	4.16 (0.44)	23.1 (5.4)	16.4 (8.0)	0.001
PCB 151	0.93 (0.06)	0.87 (0.13)	4.11 (0.53)	27.3 (7.0)	18.6 (9.3)	0.001
PCB 153/168	0.79 (0.15)	0.84 (0.12)	3.74 (0.54)	17.6 (4.1)	12.5 (6.2)	0.001
PCB 156	0.91 (0.06)	0.85 (0.09)	4.17 (0.54)	17.1 (3.8)	13.3 (6.7)	0.016
PCB 157	0.91 (0.05)	0.87 (0.12)	4.11 (0.41)	15.7 (3.6)	11.7 (5.0)	0.002

Table 2 (*Continued*)

Analyte	r^{2b}		θ (L)^c	K_fV_f ($\times 10^{-4}$ μL)^d		p^e
	Group 1	Group 2		Group 1	Group 2	
PCB 158	0.93 (0.04)	0.82 (0.12)	4.46 (0.61)	20.7 (4.9)	14.6 (7.1)	0.001
PCB 167	0.92 (0.05)	0.84 (0.13)	4.13 (0.51)	14.5 (3.1)	10.7 (4.7)	0.001
PCB 169	0.90 (0.05)	0.86 (0.11)	4.00 (0.45)	14.4 (3.0)	11.5 (5.1)	0.019
PCB 170	0.92 (0.04)	0.87 (0.11)	4.07 (0.15)	6.69 (1.97)	4.89 (1.92)	0.001
PCB 177	0.93 (0.05)	0.88 (0.10)	4.47 (0.12)	9.04 (2.68)	6.34 (2.87)	0.001
PCB 180	0.92 (0.05)	0.84 (0.15)	4.19 (0.35)	7.35 (1.96)	5.49 (2.07)	0.002
PCB 183	0.93 (0.04)	0.84 (0.14)	4.21 (0.17)	7.74 (2.21)	5.82 (2.60)	0.007
PCB 187	0.92 (0.05)	0.84 (0.15)	4.32 (0.16)	8.85 (2.48)	6.42 (2.97)	0.003
PCB 189	0.89 (0.06)	0.85 (0.12)	3.78 (0.30)	6.34 (1.48)	4.67 (1.81)	0.001
PCB 194	0.87 (0.19)	0.81 (0.22)	3.95 (0.34)	3.23 (1.04)	3.23 (1.92)	0.991
PCB 200	0.66 (0.24)	0.85 (0.17)	4.00 (0.11)	5.06 (2.64)	2.85 (0.99)	0.000
PCB 201	0.89 (0.07)	0.85 (0.22)	3.82 (0.13)	3.73 (1.16)	2.57 (0.93)	0.000
PCB 206^f	0.73 (0.26)	0.88 (0.09)	3.54 (0.11)	1.88 (0.71)	1.50 (0.80)	0.071
PCB 209^f	0.78 (0.24)	0.90 (0.11)	4.55 (0.26)	1.25 (0.58)	0.94 (78)	0.109
Aldrin	0.97 (0.03)	0.94 (0.06)	2.18 (0.96)	52.8 (13.5)	40.8 (18.7)	0.011
α-Chlordane	0.97 (0.02)	0.93 (0.05)	0.33 (0.01)	21.2 (2.6)	12.3 (5.4)	0.000
γ-Chlordane	0.96 (0.02)	0.93 (0.06)	0.44 (0.01)	23.8 (2.8)	15.5 (8.6)	0.000
Chlordene	0.97 (0.03)	0.91 (0.06)	1.12 (0.23)	36.6 (8.5)	20.3 (7.6)	0.000
Chloropyrifos	0.97 (0.04)	0.91 (0.06)	0.00 (0.00)	2.73 (0.48)	3.41 (1.22)	0.012
Diazinon	0.95 (0.04)	0.93 (0.05)	0.00 (0.00)	0.48 (0.11)	0.39 (0.16)	0.019
Dieldrin	0.98 (0.02)	0.94 (0.05)	0.23 (0.08)	5.85 (0.91)	4.61 (1.41)	0.001
Endrin	0.97 (0.04)	0.84 (0.26)	0.10 (0.02)	2.58 (0.61)	2.72 (0.62)	0.412
cis-Nonachlor	0.98 (0.02)	0.92 (0.05)	0.55 (0.04)	15.9 (1.2)	9.31 (3.66)	0.000
trans-Nonachlor	0.95 (0.03)	0.94 (0.05)	0.75 (0.00)	28.9 (4.9)	19.6 (7.8)	0.000
Oxychlordane	0.96 (0.02)	0.97 (0.02)	0.78 (0.32)	29.0 (4.2)	19.0 (10.5)	0.000
o,p'-DDD	0.98 (0.01)	0.93 (0.05)	0.34 (0.01)	13.9 (1.3)	9.69 (4.24)	0.000
p,p'-DDD	0.98 (0.02)	0.94 (0.05)	0.24 (0.01)	9.76 (0.67)	6.93 (2.55)	0.000
o,p'-DDE	0.96 (0.04)	0.90 (0.06)	1.60 (0.22)	58.2 (18.1)	27.9 (11.3)	0.000
p,p'-DDE	0.96 (0.03)	0.90 (0.05)	2.25 (0.34)	34.1 (5.4)	25.9 (9.7)	0.000
o,p'-DDT	0.95 (0.03)	0.96 (0.03)	2.11 (0.42)	31.3 (9.5)	30.1 (24.1)	0.805
p,p'-DDT	0.97 (0.03)	0.97 (0.02)	1.41 (0.12)	26.7 (6.6)	17.4 (11.2)	0.001

The number of fibers for groups 1 and 2 were 26 and 25, respectively, as three fibers were broken during SPME extraction.

^{a} The numbers in parentheses are standard errors from the linear regression analysis of the equilibrium SPME and non-SPME data.

^{b} Correlation coefficients for linear regressions on Eq. (4).

^{c} A matrix effect term defined by Zeng and Noblet [15] and obtained with Eq. (7) from five-point linear regression.

^{d} Obtained with Eq. (4) with five-point linear regression.

^{e} Probability that the K_fV_f values for groups 1 and 2 are not significantly different ($p > 0.05$).

^{f} The data are intended for qualitative assessment only due to the low aqueous solubility values for these two compounds (see text for additional discussion).

prepared standards for both instruments were used to normalize the abundances from the PDMS-coated fibers. One possibility for the discrepancy therefore is that volatilization of liquid standards did not adequately mimic the processes of desorption and volatilization from SPME fibers in the injection port, and the disparity between the direct injection and SPME was not exactly the same for the two instruments. This underscores the importance to utilize the same instrument for calibration and application of SPME fibers in the measurement of VHOCs.

For almost all the analytes, the relative standard deviations associated with the measured K_fV_f values within individual batches were smaller than the group average values (Fig. 2). The pattern was particularly prominent for low to moderately chlorinated PCB congeners with the exception of PCB 37 in one batch from group 1. A few highly chlorinated PCB congeners (e.g., PCB 194, PCB 200, PCB 206, and PCB 209) had large individual and group relative standard deviations. These results indicate that the accuracy of the calibrated K_fV_f

values was less affected by the random selection of individual SPME fibers than by other experimental conditions. As a result, average K_fV_f values may be used for the same type of commercially available SPME fibers. In general, the quality of linear regressions with group 1 is better than that with group 2 (Table 2) and the inter-batch variability with group 1 is also smaller than that with group 2 (Fig. 2). Therefore, the calibration data for group 1 will be used in the following section to compare with previously acquired data in the literature.

3.3. Comparison with previous studies

A number of studies obtained K_f values for selected PCBs and DDT compounds with PDMS-coated fibers (Table 3). Apparently, a large variability in K_f values has been obtained with different experimental procedures, PDMS coating thickness, and researchers. For example, Mayer et al. [1] obtained higher K_f values with increasing K_{ow} values with a
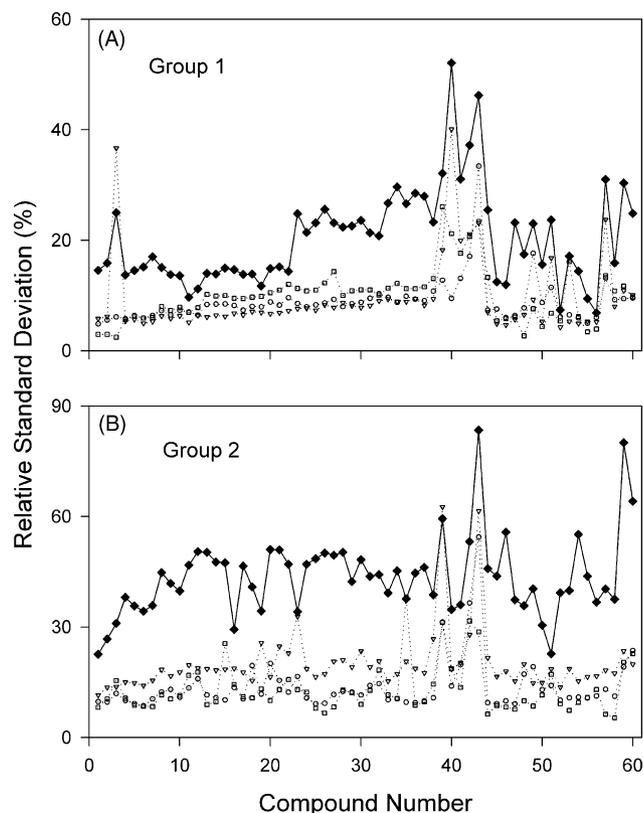
Fig. 2. Relative standard deviations (%) for measured K_fV_f values with: (A) group 1 (batches 1–3 with the number of SPME fibers being 9, 9, and 8, respectively); (B) group 2 (batches 4–6 with the number of SPME fibers being 9, 8, and 8, respectively). The compound number is in the same sequence as those displayed in Tables 1 and 2. Numbers 1–43 and 44–60 represent PCB congeners and chlorinated pesticides, respectively. (◆) Average values for the whole group; (hollow symbols) average values for individual batches (three in each group).

6-week extraction time compared to a 3-day extraction using a 15 μm coating. Sufficient equilibrium time was cited as an important factor to achieve appropriate K_f values. Poerschmann et al. [7] acquired higher K_f values with a larger sample volume (250 mL) than with a smaller one (4 mL) using a static SPME method. They were able to achieve even higher K_f values using a dynamic SPME method. More recently, Paschke and Popp [8] used a static SPME method to determine K_f on 7 and 100 μm PDMS-coated fibers in an Erlenmeyer flask (with a sample size of 480 mL). The K_f values for PCB congeners on the 7 μm PDMS-coated fibers essentially increase with increasing K_{ow} values. The K_f values for PCB congeners on the 100 μm PDMS-coated fibers also increase at low congener number with increasing K_{ow} values, but top out at log $K_{ow} \approx 6.9$ and then decrease slightly afterwards (Table 3). The log K_f values obtained in the present study using a 100 μm PDMS coating increase with increasing log K_{ow} up to log $K_{ow} \approx 6.5$, and decreases at higher log K_{ow} (Fig. 3). The log K_f value for p,p'-DDE (5.74 ± 0.07) determined in the present study is similar to those acquired by Mayer et al. [1] using a 15 μm PDMS coating (5.73 ± 0.09 and 5.88 ± 0.05 for extractions times of

3 days and 6 weeks, respectively), but quite distinct from those obtained by Paschke and Popp [8] for 7 μm (5.39) and 100 μm (5.26) PDMS coatings. Our log K_f values of p,p'-DDD and p,p'-DDT were also inconsistent with those measured by Paschke and Popp [8] and Poerschmann et al. [7] (Table 3).

While linear relationships between log K_f and log K_{ow} exist for PCBs up to log $K_{ow} \approx 7.4$ (PCB 180) for PDMS coating thickness of 7 or 15 μm [1,7,8], such linear relationships have yet to be obtained for the 100 μm PDMS coating phase. This may point to a significant relationship between the PDMS coating thickness and the permeability and sorptive capacity for molecules of different sizes. Langenfeld et al. [20] also observed a substantial difference between the K_f values with 7 and 100 μm PDMS-coated fibers for a number of PAH compounds. They noted the different procedures used to prepare the 7 and 100 μm PDMS fiber coatings by the manufacturer (Supelco), resulting in differences within the coating structures. A detailed investigation into the relationship between the physical or chemical properties of the PDMS-coated fibers and their absorption capacity for high molecular weight compounds appears necessary to understand the different absorption behavior for various PDMS coating thicknesses.

A comparison of the log K_f values from a previous study [1] and the present study can be made to assess the interlaboratory variability in calibrating SPME fibers. The present study obtained slightly larger relative standards deviations than the previous study 13 out of the 18 comparisons (Table 3). However, the differences range from 0.01 to 0.05 (log-based unit) only, representing a maximum relative error of about 13% for K_fV_f between the two studies. Therefore, the precision of the calibration methods employed by the two studies was deemed similar.

3.4. Correlation between log K_f and log K_{ow}

The correlation between log K_f and log K_{ow} for PCB congeners was similar for both groups (Fig. 3). The log K_f increases with log K_{ow} initially, but reaches a plateau at log $K_{ow} \approx 6.5$, and then decreases at higher log K_{ow}. To better demonstrate the dependence of log K_f on log K_{ow}, the PCB congeners in group 1 (Table 2) were grouped in homologs. The log K_f increases with increasing log K_{ow} for homologs 3–4 and 5, but decreases with increasing log K_{ow} for homologs 6 and 7–10. Doong and Chang [21] also reported a linear correlation between K_f and K_{ow} for polycyclic aromatic hydrocarbons (PAHs) with log K_{ow} less than 6, but obtained a negative correlation for five- and six-ring PAHs.

The curve-shaped correlation between log K_f and log K_{ow} obtained from the present study could stem from a number of factors associated with the heavily chlorinated PCBs: (1) insufficient extraction time; (2) neglect of headspace in the calibration; (3) low aqueous solubility relative to the spiking concentrations; and (4) PDMS coating thickness (i.e., steric factors).

Table 3
Comparison of experimentally measured log K_f (PDMS phase–water distribution coefficient) values

Analyte	log K_{ow}[a]	log K_f									
		Present study[b]	Mayer et al.[c]		Poerschmann et al.[d]			Yang et al.[e]		Paschke and Popp[f]	
		100 µm, 12 days	15 µm, 3 days	15 µm, 6 weeks	7 µm, 24 h		7 µm, >72 h	7 µm, 5 h	100 µm, 24 h	7 µm, 3 days	100 µm, 3days
					Static 1	Static 2	Dynamic				
PCB 18	5.24	5.11 (0.06)						4.51	4.03		
PCB 28	5.67	5.24 (0.07)			4.71	4.94	5.04	4.55	3.88	4.65	4.76
PCB 44	5.75	5.49 (0.06)						4.75	3.80		
PCB 52	5.84	5.49 (0.06)	5.30 (0.07)	5.38 (0.11)	4.48	5.21	5.55	4.67	3.87	4.98	5.14
PCB 66	6.20	5.57 (0.06)						4.85	3.88		
PCB 77	6.36	5.80 (0.04)						4.92	3.83		
PCB 101	6.38	5.61 (0.07)	5.58 (0.11)	5.71 (0.06)				4.56	3.56	5.48	5.48
PCB 105	6.65	5.73 (0.06)	5.69 (0.02)	5.89 (0.03)				3.56	3.42		
PCB 118	6.74	5.67 (0.05)	5.69 (0.06)	5.87 (0.03)	4.42	5.52	5.97	4.56	3.56		
PCB 126	6.89	5.73 (0.06)						4.52	3.22		
PCB 128	6.74	5.52 (0.10)						4.26	2.88		
PCB 138	6.83	5.49 (0.09)	5.79 (0.07)	6.20 (0.07)				4.49	3.37	5.98	5.65
PCB 153/168	6.92	5.45 (0.10)	5.84 (0.08)	6.16 (0.09)	4.41	5.63	6.05	4.57	3.42	6.01	5.67
PCB 156	7.18	5.44 (0.09)	5.79 (0.07)	6.28 (0.06)				4.21	2.92		
PCB 170	7.27	5.02 (0.13)						4.23	2.96		
PCB 180	7.36	5.07 (0.11)	5.85 (0.06)	6.40 (0.10)	4.19	5.60	6.23	4.21	2.92	6.37	5.55
PCB 187	7.17	5.14 (0.12)						4.38	3.26		
PCB 201	7.62	4.77 (0.12)						4.23	3.08		
PCB 206	8.09	4.46 (0.17)						3.79	2.45		
PCB 209	8.18	4.27 (0.20)						3.75	2.43		
p,p'-DDE	6.96	5.74 (0.07)	5.73 (0.09)	5.88 (0.05)						5.39	5.26
p,p'-DDD	6.22	5.20 (0.03)								4.45	4.55
p,p'-DDT	6.91	5.63 (0.10)					5.33[g]				

All data were acquired with static SPME methods except for those by Poerschmann et al. [7] as indicated.

[a] The PCB and DDT data were obtained from Hawker and Connell [30] and de Bruijn et al. [31], respectively.

[b] Extracted from the group 1 data in Table 2.

[c] Extracted from Mayer et al. [1] with the numbers in parentheses being standard deviations; water volume was 1 L with an initial concentration of 100 ng/L.

[d] Extracted from Poerschmann et al. [7]; initial concentration of 50 ng/L and 4 mL sample volume were employed for static 1 and initial concentration of 500 ng/L and a 250 mL sample volume for static 2 employed; constant analyte concentrations were maintained during the dynamic experiments.

[e] Extracted from Yang et al. [12]; sample volume was 2 mL and initial analyte concentration was 50 ng/L.

[f] Extracted from Paschke and Popp [8].

[g] Only DDT was indicated in the paper [7].

E.Y. Zeng et al. / J. Chromatogr. A 1066 (2005) 165–175

173
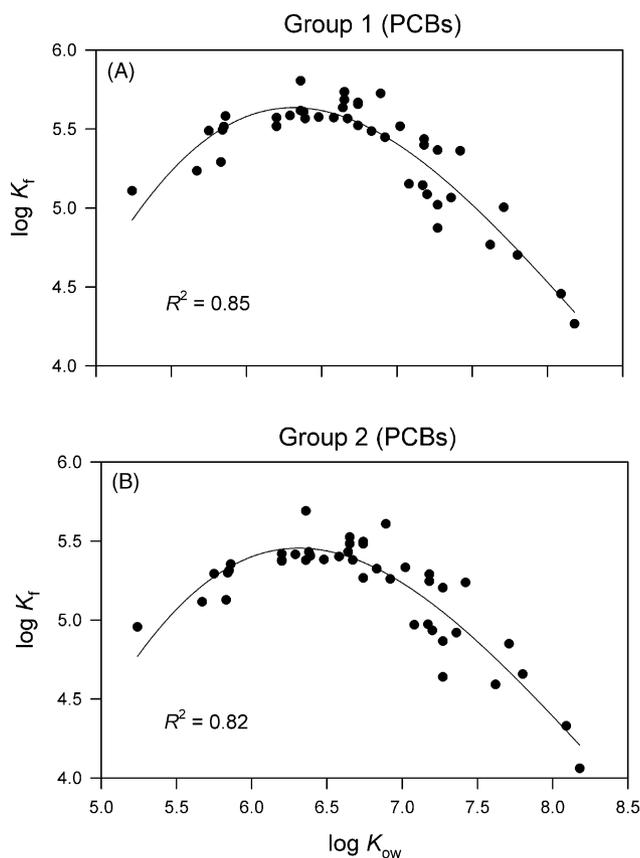
Group 1 (PCBs)

Group 2 (PCBs)

Fig. 3. Correlation of measured $\log K_f$ and $\log K_{ow}$ for polychlorinated biphenyls (PCBs) with: (A) group 1; (B) group 2. The $\log K_{ow}$ values were obtained from Hawker and Connell [30].

In consideration of all the above factors, insufficient extraction time was deemed unlikely as the cause for the nonlinearity. In order to produce a linear relationship, the K_f values would need to increase by as much as one to two orders magnitude. This is not possible if the results of the nonlinear regression of the kinetic data are valid. A qualitative inspection of the kinetic data (not shown) shows that all congeners have passed the steep part of the sorption growth curve, and are asymptotically approaching equilibrium. This is consistent with the calculated P_{ES} values that were generally $\geq 82\%$ (Table 1). Even in the worst case of PCB 209 ($P_{ES} = 66\%$), extrapolation to a P_{ES} value of 100% does not account for the deviation from linearity. Moreover, these conclusions are supported by the marginal increases observed in the experimental data when the extraction time was doubled to 24 days. While small increases in K_f values would certainly be achieved through prolonged extraction times, practical considerations, especially for field deployment, outweigh any gain in analytical sensitivity.

The effect of neglecting headspace on the $K_f V_f$ values can be assessed by comparing the values of $K'_H V_a$ and $V_w + \theta$ in Eq. (5). In the present study, the ratio of V_a/V_w was ~ 0.04 and θ was about 4 L for hexachlorobiphenyl or heavier PCBs (Table 2). As an example, a Henry's Law constant of 100 Pa m^3/mol at 22 °C would lead

to $K'_H V_a \sim 1.6 \times 10^{-3} V_w$. A different but equivalent way to evaluate the headspace effect is to estimate the ratio (N_a/N_w) of the analyte amounts in the air and aqueous phases when equilibrium is established. The N_a/N_w value is ~ 0.0016 for an analyte with a Henry's Law constant of 100 Pa m^3/mol at 22 °C. The Henry's Law constants reported in the literature are quite variable for a given chemical. Nevertheless, a comparison of several sources [22–24] indicates that the Henry's Law constants for our target analytes (both PCBs and chlorinated pesticides) are mostly between 1 and 100 Pa m^3/mol. The above assessment suggests that neglect of headspace did not contribute significantly to the nonlinearity.

Low solubility could affect the determination of $K_f V_f$ in both the SPME and non-SPME experiments. Unfortunately, a quantitative assessment is complicated because of the large variability in any available solubility data. For example, in the case of DDT and DDE, Pontolillo and Eganhouse [25] could not identify any solubility dataset that met their highest rating criteria. Therefore, any implications from the present assessment are deemed qualitative and tentative. An examination of compiled solubility data [22–24] indicates that solubility was likely a significant factor only for PCB 206 and PCB 209, with aqueous solubilities of 25 and 1 ng/L [23], respectively. These solubilities are similar to the spiking concentrations (2, 5, 20, and 50 ng/L) for the SPME calibration experiments, and significantly lower than the spiking concentrations of 100, 200, 500, and 1000 ng/L for the non-SPME experiments. However, the actual impact on the resulting K_f data was deemed moderate for the following reason. The loss of a fraction of the analyte from the dissolved phase due to precipitation would lead to two competing consequences for the SPME and non-SPME experiments. For SPME experiments, the consequence would be a decrease of the S value and therefore a lower $K_f V_f$ (Eq. (5)). In non-SPME experiments, this lost fraction would be collected in a non-SPME sorbent phase (i.e., glassware wall and/or stirring bar surface), resulting in an increase of the θ value (Eq. (7)) and consequently an increase of $K_f V_f$. More importantly, the curve-shaped correlation between $\log K_f$ and $\log K_{ow}$ (Fig. 3) would remain intact even if the data points for PCB 206 and PCB 209 (the last two points at the high end of the $\log K_{ow}$ scale) were removed. Solubility was not an issue for determination of $K_f V_f$ for chlorinated pesticides because of their higher aqueous solubilities.

Elimination of the other factors lead to the conclusion that the PDMS coating thickness was most significant in affecting the sorptive capacity for PCB congeners of different sizes as discussed in the preceding section. The effect of PDMS coating thickness can be considered analogous to the steric effects that have long been recognized for bioconcentration of PCBs and other hydrophobic chemicals in aquatic species [26,27]. Recently, Kraaij et al. [28] argued that equilibrium partitioning theory is a conceptually correct representation of sediment bioaccumulation (i.e., no steric effects) for hydrophobic organic compounds up to $\log K_{ow}$ 7.5 only if the rapidly desorbing fraction of hydrophobic organic compounds is included in the sorbent phase equilibrating with sediment pore-

water. Clearly, further research is needed to confirm and clarify the importance of steric effects on the mechanism of sorption with SPME. A radiochemical technique would likely be appropriate for this task [29].

References

[1] P. Mayer, W.H.J. Vaes, J.L.M. Hermens, Anal. Chem. 72 (2000) 459.
[2] C.L. Arthur, J. Pawliszyn, Anal. Chem. 62 (1990) 2145.
[3] J. Pawliszyn, Solid Phase Microextraction: Theory and Practice, Wiley–VCH, New York, 1997.
[4] J. Pawliszyn, Applications of Solid Phase Microextraction, Royal Society of Chemistry, Cambridge, UK, 1999.
[5] P. Mayer, J. Tolls, L. Hermens, D. Mackay, Environ. Sci. Technol. 37 (2003) 184A.
[6] M.B. Heringa, J.L.M. Hermens, TrAC Trends Anal. Chem. 22 (2003) 575.
[7] J. Poerschmann, T. Górecki, F.-D. Kopinke, Environ. Sci. Technol. 34 (2000) 3824.
[8] A. Paschke, P. Popp, J. Chromatogr. A 999 (2003) 35.
[9] B. Shurmer, J. Pawliszyn, Anal. Chem. 72 (2000) 3660.
[10] E.Y. Zeng, D. Tsukada, D.W. Diehl, Environ. Sci. Technol. 38 (2004) 5737.
[11] Y. Yang, D.J. Miller, S.B. Hawthorne, J. Chromatogr. A 800 (1998) 257.
[12] Y. Yang, S.B. Hawthorne, D.J. Miller, Y. Liu, M.L. Lee, Anal. Chem. 70 (1998) 1866.
[13] D.W. Potter, J. Pawliszyn, Environ. Sci. Technol. 28 (1994) 298.
[14] J.A. Noblet, E.Y. Zeng, R.W. Gossett, C.R. Phillips, R.J. Ozretich, R. Baird, Southern California Coastal Water Research Project, Westminster, CA, 2002.
[15] E.Y. Zeng, J.A. Noblet, Environ. Sci. Technol. 36 (2002) 3385.
[16] E.Y. Zeng, A.R. Khan, J. Microcolumn Sep. 7 (1995) 529.
[17] E.Y. Zeng, C. Vista, Environ. Toxicol. Chem. 16 (1997) 179.
[18] J. Ai, Anal. Chem. 69 (1997) 1230.
[19] J.N. Cross (Ed.), Southern California Coastal Water Research Project, Annual Report 1992–1993, Westminster, CA, 1994, p. 75.
[20] J.J. Langenfeld, S.B. Hawthorne, D.J. Miller, Anal. Chem. 68 (1996) 144.
[21] R.-A. Doong, S.-M. Chang, Anal. Chem. 72 (2000) 3647.
[22] D. Mackay, W.Y. Shiu, K.C. Ma, Illustrated Handbook of Physical–Chemical Properties and Environmental Fate for Organic Chemicals. Monoaromatic Hydrocarbons, Chlorobenzenes, and PCBs, vol. I, Lewis Publishers, 1992.
[23] W.Y. Shiu, K.C. Ma, J. Phys. Chem. Ref. Data 29 (2000) 387.
[24] Agricultural Research Service (United States Department of Agriculture), http://www.arsusda.gov/acsl/services/ppdb/ppdb3.html, Access date: July 2004.
[25] J. Pontolillo, R.P. Eganhouse, U.S. Geological Survey, Water-Resources Investigations Report 01-4201, Reston, VA, 2001.
[26] G.R. Shaw, D.W. Connell, Chemosphere 9 (1980) 731.
[27] A. Opperhuizen, E.W.v.d Velde, F.A.P.C. Gobas, D.A.K. Liem, J.M.D.v.d. Steen, Chemosphere 14 (1985) 1871.
[28] R. Kraaij, P. Mayer, F.J.M. Busser, M.V.H. Bolscher, W. Seinen, J. Tolls, A.C. Belfroid, Environ. Sci. Technol. 37 (2003) 268.
[29] M.B. Heringa, D. Pastor, J. Algra, W.H.J. Vaes, J.L.M. Hermens, Anal. Chem. 74 (2002) 5993.
[30] D.W. Hawker, D.W. Connell, Environ. Sci. Technol. 22 (1988) 382.
[31] J. de Bruijn, F. Busser, W. Seinen, J. Hermens, Environ. Toxicol. Chem. 8 (1989) 499.